Performance evaluation of coarse-graded field mixtures using dynamic modulus results gained from testing in indirect tension mode of testing

by

Parnian Ghasemi

A thesis submitted to the graduate faculty

in partial fulfillment of the requirements for the degree of

MASTER OF SCIENCE

Major: Civil Engineering (Civil Engineering Materials)

Program of Study Committee:
R. Christopher Williams, Major Professor
Vernon R. Schaefer
Derrick K. Rollins

The student author, whose presentation of the scholarship herein was approved by the program of study committee, is solely responsible for the content of this thesis. The Graduate College will ensure this thesis is globally accessible and will not permit alterations after a degree is conferred.

Iowa State University

Ames, Iowa

2018

DEDICATION

For my parents,

even though they did not want me to become a CIVIL engineer!!

TABLE OF CONTENTS

Page

LIST OF FIGURES

Page

LIST OF TABLES

Page

NOMENCLATURE

HMA	Hot Mix Asphalt
ANN	Artificial Neural Network

ACKNOWLEDGMENTS

I would like to thank my committee members, Dr. Christopher Williams, Dr. Vernon Schaefer, and Dr. Derrick Rollins, for their guidance and support throughout the course of this research.

In addition, I would also like to thank my friends, colleagues, the department faculty and staff for making my time at Iowa State University a wonderful experience. I want to also offer my appreciation to those who were willing to participate in my surveys and observations, without whom, this thesis would not have been possible.

ABSTRACT

Historically, asphalt mixtures in Minnesota have been produced with fine gradations. However, recently more coarse-graded mixtures are being produced as they require less asphalt binder. Thus, it is important that pavement performance for coarse gradations be evaluated. It is of critical importance to obtain the dynamic modulus of asphalt pavements under repetitive traffic loading to predict its performance and service life. The indirect tension mode can measure the dynamic modulus of each layer of field cores without the dimensional requirement, e.g. a height of 6-inch is required for the traditional uniaxial test mode. Within this research work, performance evaluation took place with the use of the Dynamic Modulus Test in Indirect Tension mode on coarse-graded mixtures consisting of field cores from 9 different pavements located in five districts of Minnesota. From each pavement's surface layer, 3 specimens were tested at three temperatures; 0.4°C, 17.1°C, and 33.8°C each at nine frequencies ranging between 0.1 Hz and 25 Hz. Additional volumetric characterization of the field mixtures was done to determine asphalt content, air voids, and blended aggregate gradations. Asphalt binders were extracted and recovered for use in determining binder shear complex master curves. Through this information the modified Witczak model was used to create $|E^*|$ master curves which were then compared against the indirect tension (IDT) test $|E^*|$ experimentally created master curves. According to the results the Modified Witczak Model needs to be modified for IDT collected dynamic modulus data.

Another focus of this research is developing an accurate finite element (FE) model using mixture elastic modulus and asphalt binder properties to predict dynamic modulus of asphalt concrete mix in indirect tension mode. An Artificial Neural Network is used to back-calculate the elastic modulus of asphalt mixtures. The developed FE model was verified against experimental results of field cores from nine different pavement sections from five districts in Minnesota. It is demonstrated that the ANN modeling is a powerful tool to back-calculate the elastic modulus and FE model is capable of accurately predicting dynamic modulus.

CHAPTER 1. INTRODUCTION

Understanding of the stress-strain behavior of pavement materials under repetitive traffic loading is necessary to predict the pavement performance and service life. Dynamic modulus relates stress to strain for a linear viscoelastic material subjected to sinusoidal loading, and can be determined by applying sinusoidal loads in a range of selected frequencies to hot mix asphalt (HMA) samples while measuring the deformation. Dynamic modulus represents the frequency/time dependent stiffness characteristic of the material, and has become the main input property of HMA in the Mechanistic-Empirical Pavement Design Guide (MEPDG) and has gained more attention recently (Witczak and El-Basyouny 2004).The dynamic modulus test has been studied since the 1960's (Raad and Figueroa 1980) and was accepted as a standard test method in 1979 and was reapproved in 1995 (ASTM D 3497-79 1995). The dynamic modulus test is accepted by pavement agencies as a critical parameter for pavement design and a dynamic modulus master curve for asphalt concrete is an important input for flexible pavement design in the mechanistic-empirical pavement design guide developed in NCHRP Project 1-37A (Kim, et al., 2004).

The dynamic modulus $\left|E^*\right|$ is calculated by dividing the stress amplitude by the strain amplitude in a steady state response as presented in equations (1) and (2) below.

$$\boldsymbol{E^*} = \frac{\boldsymbol{\sigma}}{\boldsymbol{\varepsilon}} = \frac{\boldsymbol{\sigma_0}.\boldsymbol{e^{i\omega t}}}{\boldsymbol{\varepsilon_0}.\boldsymbol{e^{i(\omega t-\delta)}}} = \frac{\boldsymbol{\sigma_0}.\mathbf{sin}(\boldsymbol{\omega t})}{\boldsymbol{\varepsilon_0}.\mathbf{sin}(\boldsymbol{\omega t}-\boldsymbol{\delta})} \quad (1)$$

$$|E^*| = \frac{\sigma_{amp}}{\varepsilon_{amp}} = \frac{\sigma_0}{\varepsilon_0} \quad (2)$$

where $|E^*|$= dynamic modulus; E^* = complex modulus; σ_0= peak (maximum) stress; ε_0 = peak (maximum) strain; δ = phase angle, degrees; ω = angular velocity; t = time,

seconds; *e* = exponential; and *i* = imaginary component of the complex modulus (Dougan *et al.* 2003),(Schwartz 2005).

Dynamic modulus testing should be performed over a range of test temperatures (e.g. -10 to 54.4 °C) and frequencies (e.g. 0.1 to 25 Hz) to measure the viscoelastic response of the asphalt concrete. The temperatures and frequencies are used to create a master curve in order to exhibit the properties of the mixture over a wide range of temperatures and frequencies (AASHTO T 342-11 2012), (AASHTO TP 79-13 2013). A master curve for materials which comply with the time-temperature superposition principle (TTSP) is a continuous shape used to interpret complex modulus test results with horizontal shifting of the measured dynamic modulus and phase angle data at different temperatures with respect to a pre-selected temperature.(Mitchell *et al.* 2008)

The dynamic modulus test is performed based on the current test protocol, AASHTO T 342-11 (AASHTO T 342-11 2012), which is used for the uniaxial compression testing of 4-inch (101.6-mm) diameter and 6-inch (152.4-mm) tall asphalt concrete specimens. One of the issues related to the role of the dynamic modulus in pavement management is its use in forensic studies and pavement rehabilitation design. It is often impossible to obtain 4-inch (101.6-mm) diameter and 6-inch (152.4-mm) tall asphalt concrete specimens from individual pavement layers to use in dynamic modulus testing, because many asphalt layers are less than a few inches thick (Kim *et al.* 2004). Another challenge is designing asphalt mixes in a multi-layered system. These layers have different aggregate gradations, binder contents, and stiffness, so they commonly have different dynamic modulus values. In the uniaxial dynamic modulus test this difference is often not considered, but it is possible to measure layers' dynamic modulus values separately using an indirect tension test (IDT) mode and evaluating

a layer's performance using the obtained moduli. Therefore, the IDT is an excellent candidate to be more practical for the evaluation of dynamic modulus of field cores (Ghasemi *et al.* 2016).

The IDT dynamic modulus test protocol was evaluated by Kim (Kim *et al.* 2004), using 6-inch (152.4 mm) diameter, 1.5-inch (38.1 mm) thick specimens cut from Superpave gyratory compacted (SGC) specimens. Sinusoidal loading is applied in a controlled stress mode. Horizontal and vertical deformations are measured from two loose core type miniature linear variable differential transformers (LVDT) with a 50.8-mm (2-inch) gauge length located on each side of a specimen's face. Figure 1.1 represents the IDT dynamic modulus test setup with a 6-inch (152.4-mm) diameter specimen and four LVDTs connected to the specimen. Based on the AASHTO T342-11(AASHTO T 342-11 2012) specification, testing must take place on at least two replicate specimens at five temperatures between 14°F and 130 °F (-10 °C and 54.4 °C) and at six frequencies between 0.1 and 25 Hz (AASHTO T 342-11 2012).

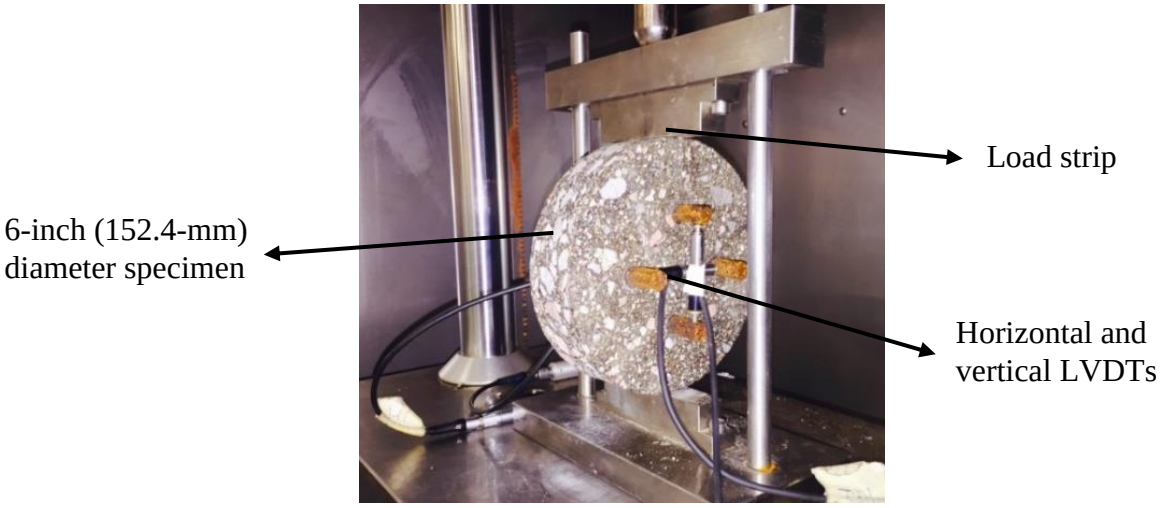

Figure 1.1 IDT dynamic modulus test setup

Due to the number of temperatures this specification is time consuming and costly. In a recent study Li and Williams (2015) found that five test temperatures are not necessary to build an accurate, and smooth master curve. From this study it was found that with three temperatures and nine frequencies an equivalent master curve comparable to one made using results from testing at five temperatures and six frequencies could be developed (Li and Williams 2015).

Elastic solutions for the IDT test has been studied by Hondros (Hondros 1959), with Roque and Buttlar making some corrections by considering the bulging effect of the specimen (Kim *et al.* 2004). A viscoelastic solution for the IDT creep test was introduced by Kim and Wen (Kim and Wen 2002). In the IDT test mode, the specimen stress-strain distribution is biaxial, and for a viscoelastic material subjected to sinusoidal loading in a steady state the relationship between strain and biaxial stress can be defined as shown in equation 3 (Kim *et al.* 2004).

$$\boldsymbol{\varepsilon_x = \frac{1}{E^*}\left(\sigma_x - \nu\sigma_y\right)} \tag{3}$$

where E^* = the complex modulus; ε_x = horizontal strain; ν = Poisson's ratio; and $(\sigma_x - \nu\sigma_y)$= the biaxial stress. In other words, the complex modulus can be obtained by dividing the biaxial stress by the horizontal strain.

$$\boldsymbol{E^* = \frac{\left(\sigma_x - \nu\sigma_y\right)}{\varepsilon_x}} \tag{4}$$

The MEPDG uses a mastercurve and time-temperature shift factors in its internal computations. The mastercurve is constructed based on a hierarchical structure of inputs obtained from laboratory testing on HMA specimens. There are some cases in which the $|E^*|$ values for materials used in a specific design might not be available when the analysis is

performed. In such cases, one may choose to utilize a predictive equation based on mixture volumetric and aggregate and asphalt binder properties in order to predict the mixture modulus. For this purpose several predictive models have been developed among them, Witczak model, Hirsch model, modified Witczak model and Al-Khateeb model (which is a modified form of Hirsch model) are the most well-known ones. Although various researchers have used and reviewed these models for test data obtained from uniaxial mode of testing, no attempts have been made on examining these models using data obtained from indirect tension mode of testing.

Despite all of the benefits mentioned previously, the dynamic modulus test in indirect tension mode has some limitations. The probability of getting damaged by the specimen specially at higher temperatures is pretty high. The pre-testing (tuning) process increases the testing time and needs a reasonable attention in order to hold the strain in the allowable range. Also using LVDTs can cause errors in measuring the corresponding deformation, which affects the modulus. All of these obstacles provide motivation for researchers to find a replacement for this test configuration, in order to reduce the test effort and provide results with lower variability. Researchers considered changing the sample geometry in order to measure a layer modulus using the uniaxial test configuration. Although it can help reduce the likelihood of specimen damage it still needs much effort for trimming specimens out of field cores. In addition, the measurement errors due to using LVDTs still exist (Lin *et al.* 2016). The best way to overcome all of the barriers is using the application of FE analysis in the modulus calculation.

It has been shown that the FE method is a powerful tool to simulate the viscoelastic behaviour of asphalt mixtures (Williams *et al.* 2009). However, there is no effort to use the

application of FE modelling to simulate and further understanding of the dynamic modulus test in the indirect tension mode. Therefore, one objective of the present research is to illustrate using the application of FE modelling to predict dynamic modulus value of asphalt concrete. Secor and Monismith were the first ones who studied asphalt as a viscoelastic material (Herzog *et al.* 2008) and Duncan was the first researcher who used the application of FE analysis using elastic theory (Duncan and M.C 1968). Owen and Hinton developed a two-dimensional FE analysis program based on springs and dashpots (Lytton *et al.* 1993). Lytton developed a similar two-dimensional FE program with a modification based on a viscoelastic model. During the 1980s, two main FE programs were developed: ILLI-PAVE and MICH-PAVE (Witczak *et al.* 2002). Collop developed a FE program entitled CAPA-3D using the viscoelastic model to determine the stress of specific element due to loading (Collop *et al.* 2003). FE analysis method has been used by Elseifi et al. to compare the material response with modelling the material as an elastic or viscoelastic (Elseifi *et al.* 2006). They found that viscoelastic simulation provides a more accurate estimate to the pavement response.

Predictive modelling is a process that can use data mining tools and probability theory techniques to forecast outcomes from a given system, with each model constructed with several likely to influence future results. Once the data have been collected for relevant predictors, a statistical model formulated that may use a simple linear regression or may rather use a more complicated pattern recognition technique (Ghasemi *et al.* 2018). Modern pattern recognition techniques can learn and recognize trends in data contributing to their current widespread use. These techniques learn the pattern from experimental data and design the computational models. One such approach, Artificial Neural Network (ANN), is an interconnected network of many simple processors (nodes). All ANNs consist of a set of

processing units or neurons classified as input, hidden and output neurons. Input neurons receive input from external sources and transfer it to the rest of the network. Hidden neurons receive input and transmit their computed output to the processing units within the network without any outside contact. Output neurons receive the input from the rest of the network that it transforms and sends to external receivers (Kartam 1994).

In the present study, the dynamic modulus test in IDT mode was performed at three temperatures (0.4, 17.1, and 33.8 °C) each at nine frequencies (25, 20, 10, 5, 2, 1, 0.5, 0.2, and 0.1 Hz). Linear viscoelastic theory has been used which considers time rate of stress and strain in the asphalt concrete (Akbulut and Aslantas 2005). Among all of the existing predictive models modified Witczak model has been selected to evaluate whether this predictive model compares well against the experimentally shifted dynamic results. It is assumed that the asphalt concrete is homogenous and isotropic with the same modulus values in both tension and compression. Experimental laboratory data are used as well as ANN modelling to provide input data for the FE analysis.

CHAPTER 2. MATERIALS AND METHODOLOGIES

Within this research work, field cores from nine different pavement sections were collected across five districts in the State of Minnesota. From each pavement's surface layer, three specimens were used for testing. A summary of each of these nine pavement sections information is presented in Figure 2.1 and Table 2.1.

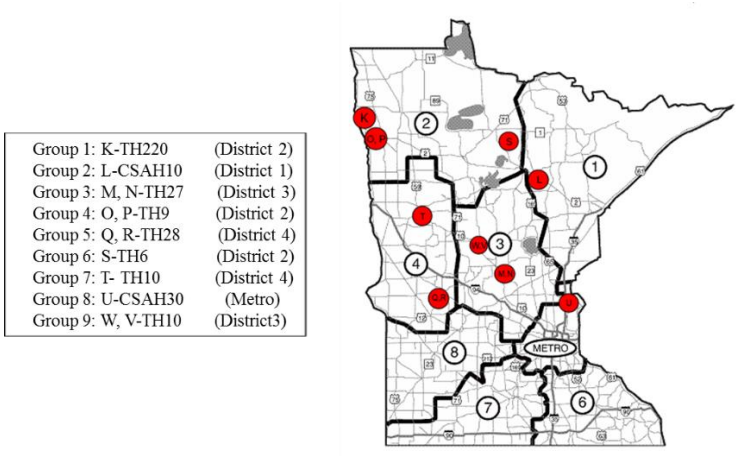

Figure 2.1 Locations of Pavement Sections in Minnesota

Table 2.1 Pavement section information

Group No.	Section	MnDOT District	Construction Year	Construction Type
1	TH 220	2	2012	3" M/O*
2	CSAH 10	1	2012	1.5" O/L** on old AC
3	TH27	3	2010	3" M/O
4	TH 9	2	2011	3" O/L on reclaimed AC
5	TH 28	4	2012	4.5" M/O
6	TH 6	2	2010	1.5" M/O
7	TH 10	4	2013	3.5" M/O
8	CSAH 30	Metro	2012	6" M/O
9	TH 10	3	2005	4" M/O (sealed cracks)
10	TH 10	3	2005	4" M/O (cracks not sealed)

* M/O = Mill and Overlay; ** O/L = Overlay

Specimens are 6 inches (152.4-mm) in diameter and about 1.5-inches (38.1-mm) in thickness. Volumetric properties of asphalt mixtures have been determined to be used in future modelling.

Dynamic Modulus Testing

The dynamic modulus $|E^*|$ is a complex number that describes the relationship between stress and strain for a linear viscoelastic material under sinusoidal loading, and it is defined as the ratio of amplitude of the sinusoidal stress and sinusoidal strain in a steady state response.

The dynamic modulus is a performance related property that can be used for mixture evaluation and characterizing the stiffness of hot mix asphalt (HMA) for use in mechanistic-empirical pavement design. The indirect tension (IDT) mode dynamic modulus test protocol was evaluated by Kim (Kim, et al., 2004) using 6-inch (152.4 mm) diameter, 1.5-inch (38.1 mm) thick specimens cut from Superpave gyratory compacted (SGC) specimens. Sinusoidal loading is applied in controlled stress mode. Horizontal and vertical deformations are measured from two loose core type miniature linear variable differential transformer (LVDT)s with a 50.8mm gauge length located on each side of a specimen's face. Based on the AASHTO TP 62-07 specification, testing must take place on at least two replicate specimens at five temperatures between 14°F and 130°F (-10°C and 54.4°C) and six loading rates between 0.1 and 25 Hz. In order to remain linear viscoelastic, Kim presented a linear viscoelastic solution and calculated coefficient for Poisson's ratio and dynamic modulus for different specimen diameters and gauge lengths. Based on these results the target horizontal tensile stain is 40-60 microstrains and the target vertical compressive strain should be under 100 microstrains (Kim et, al. 2004).

One of the important parameters used in Mechanistic-Empirical pavement design for

asphalt concrete is the dynamic modulus. This property represents the temperature and frequency-dependent or time-dependent stiffness characteristic of the pavement material. It is used in the AASHTOWare Pavement ME to determine the temperature and rate-dependent behavior of an asphalt concrete layer. For this study, the dynamic modulus test in IDT mode will be performed at three temperatures (0.4°C, 17.1°C, and 33.8°C each at nine frequencies (25, 20, 10, 5, 2, 1, 0.5, 0.2, and 0.1 Hz).

In order to obtain binder properties for each pavement group, binder extraction was done (ASTM D7906-14 2014). The extracted binder then was recovered for testing (ASTM D2172 2011). A random number generator which generates numbers between one and three was used to pick one sample from each pavement section to do the binder extraction and recovery from the randomly chosen specimen. Some of the other mix properties including binder content, air voids etc., for all of the nine pavement sections are summerized in Table 2.2.

Table 2.2 Mix properties

Mix property	Group No.	1	2	3	4	5	6	7	8	9
	% RAP	23.8	23.3	37.2	26.2	23.8	36.4	23.3	11.4	45.3
	% AC	4.5	5.2	5.6	4.8	4.8	4.9	5.6	5.3	5.0
	% V_{beff}	4.2	4.1	4.1	3.9	3.5	4.3	4.2	4.0	4.6
	%VMA	13.5	13.5	13.6	13.1	12.5	13.9	13.7	13.4	14.4
	% VFA	70.3	70.4	70.6	69.6	68.1	71.2	70.8	70.2	72.3
	G_{mb}	2.315	2.315	2.315	2.315	2.315	2.315	2.315	2.315	2.315
	G_{mm}	2.406	2.458	2.510	2.479	2.635	2.458	2.479	2.510	2.437
	% V_A	4.010	3.996	3.998	3.982	3.988	4.003	4.000	3.993	3.989

Complex shear modulus (G*) have been determined using a Dynamic Shear Rheometer (DSR) for the recovered binders from all nine mixes (Standard Test Method for Determining the Complex Shear Modulus (G *) Of Bituminous Mixtures Using Dynamic Shear Rheometer 2016).

Modified Witczak Model

The modified Witczak model is a semi-empirical method used for asphalt concrete dynamic modulus estimation. It is based on nonlinear regression and was formulated through historical data taken from 346 mixtures (7,400 data points). This model was made in response to the limitations identified by the original Witczak model (Bari and Witczak, 2006, Witczak, et al., 1999). A main limitation of the original Witczak model was its dependence on needing other models to convert binder complex shear modulus values into binder viscosity. Furthermore, the original model was not sensitive to changes in volumetrics such as voids in the mineral aggregate (VMA), voids filled with asphalt (VFA), binder content and air voids. Some of these limitations are addressed in the modified model through use of the following parameters: V_a = percentage of air voids (by volume of mix), V_{beff} = percentage of effective binder content (by volume of mix), $|G_b^*|$= complex shear modulus of binder (psi), and δ_b= phase angle of binder associated with$|G_b^*|$(degrees). The modified Witczak model is shown below in Equation 5 (Bari and Witczak, 2006).

$$\log_{10}\left|E^*\right| = -0.349 + 0.754(|G_b^*|^{-0.0052}) \times \left(6.65 - 0.032\rho_{200} + 0.0027\rho_{200}^2 + 0.011\rho_4 - 0.0001\rho_4^2 + 0.006\rho_{38} - 0.00014\rho_{38}^2 - 0.08V_a - 1.06\left(\frac{V_{beff}}{V_a+V_{beff}}\right)\right) + \frac{2.56+0.03V_a+0.71\left(\frac{V_{beff}}{V_a+V_{beff}}\right)+0.012\rho_{38}-0.0001\rho_{38}^2-0.01\rho_{34}}{1+e^{(-0.7814-0.5785\log|G_b^*|+0.8834log\delta_b)}} \quad (5)$$

where, $|E^*|$ = dynamic modulus (psi), ρ_{200} = percentage of aggregate passing no. 200 sieve, ρ_4 = percentage of aggregate retained on no.4 sieve, $\rho_{3/8}$ = percentage of aggregate retained on no.3/8" sieve, and $\rho_{3/4}$ = percentage of aggregates retained on no.3/4" sieve.

As part of this study the E* values are predicted using G_b* values, and volumetrics using the Modified Witczak Model. As such, the predicted E* values will be compared with laboratory results to see how well the Modified Witczak Model compares against experimental data gained in the IDT mode for dynamic modulus testing.

Finite element analysis

FE analysis was performed using a multi-purpose FE software, ABAQUS ™ version 6.14.2 (Documentation, Abaqus. 'Version 6.14-2.' 2014). ABAQUS has a module for viscoelastic materials which can be used in modeling asphalt concrete. A FE model was then developed using the results from the complex shear modulus test and was calibrated using the dynamic modulus for the IDT mode test results. A model with cylindrical geometry having the same dimensions as the IDT dynamic modulus specimen is used in this study.

Material characterization

There are several ways of defining the material properties in the ABAQUS. The complex shear modulus test results were used in this analysis. Temperature dependency of the material had to be defined in the model (Breakah and Williams 2013). Temperature dependency is calculated using the shift factors obtained from the Williams-Landel-Ferry (WLF) equation (Williams *et al.* 1955),(Brinson and Brinson 2015).

$$\log \alpha_T = \frac{C_1 (T - T_S)}{C_2 + T - T_S} \quad (6)$$

where C_1 and C_2 =constants; T_S = the reference temperature; and T = the temperature of each individual test. The reference temperature is assumed to be 17.1 ° C in this research. The simulation is then repeated for other two temperatures, 0.4 ° C and 33.8 ° C. For each individual temperature, after determining C_1 and C_2 and shifting all of complex modulus data to this reference temperature, the value of these two constants at the reference temperature were put into the model as inputs. ABAQUS has a built-in function which transforms the shear modulus into a Prony series which is an exponential expansion often used to describe the relaxation modulus of a viscoelastic material (Brinson and Brinson 2015). The data is entered as long term modulus and then normalized as the ratio of the modulus at individual times to the long term modulus. The Poisson's ratio was assumed to be 0.25. The selection of this values was based on material behavior at 17 °C. A sensitivity analysis on the Poison's ratio impact on the dynamic modulus values was conducted and the results demonstrated that a very negligible effect exists. In order to define the elastic behavior of the asphalt mixture in the absence of the field data, a neural network algorithm is used to obtain the modulus for using in the FE model.

Back-calculation of the elastic modulus of asphalt mixture using Artificial Neural Network

In order to simulate the viscoelastic behavior of asphalt mixture, both viscous and elastic properties of the material should be defined in the ABAQUS (Breakah *et al.* 2009). In the present study, the elastic modulus is used to represent the elastic behavior of the asphalt mixture. The interconversion method between linear viscoelastic material properties

(Schapery and Park 1999), is used and presented by equation 6 in which the dynamic modulus is converted into the storage modulus.

$$\boldsymbol{E' = |E^*| \cos \phi} \quad (7)$$

where E' = the storage modulus; $|E^*|$ = the dynamic modulus, and ϕ = the phase angle. The storage modulus is an indicator of elastic behavior of the material and is an estimation of the elastic modulus.

To provide a larger data set of elastic modulus, the laboratory test results of dynamic modulus at different temperatures and loading frequencies for 20 different mixes from the States of Iowa, Minnesota and Wisconsin are used to calculate the elastic modulus.

An artificial neural network is then used for back-calculating the elastic modulus. An artificial neural network is an interconnected collection of processing elements (Saltan *et al.* 2002). The network can be trained to approximate a complex, nonlinear function through repeated exposure to produce meaningful solutions to problem, (Saltan and Sezgin 2007), (Aslani and Asla 2010), (Rahami *et al.* 2011). One of the most useful applications of neural networks is in back-calculation procedures, where it can be trained to approximate the inverse function by repeatedly showing it forward problem solutions. Once a network learned the pattern of inputs/outputs relationship, it can predict new conditions (Kartam, Nabil. Flood 1994).

A basic network is typically composed of three or more layers. The first and last layers contain the input data and output results, respectively. One or more hidden layers are placed between the input and output layers.

The hidden layers designate and learn the patterns qualifying the data presenting the network. The multilayer architecture of the neural network ensures nonlinear mapping of

input to output. There is no standard technique to get the optimum number of hidden layers. So, a number of alternative neural networks are chosen with different hidden layers and 10 neurons in each layer are tested for their training speed to finally obtain a suitable network to be used for this particular study in terms of the minimum mean squared error, the maximum r-fit value and optimum training speed. The variables are the number of hidden layers, the number of neurons in each hidden layer, the maximum number of cycles, and the learning rate. For a given category of a back-calculation problem, 10 to 15 neurons in the hidden layer are chosen, depending on whichever configuration provides the best result within that category. The numbers of neurons for input and output layers are fixed.

In the current study, a three-layer feed-forward error-back propagation network composed of an input layer, an output layer, and one hidden layer was developed using MATLAB program (MATLAB 2012). Figure 2.2 presents a schematic architecture of an ANN with 8 neurons in the input layer, 10 neurons in the hidden layer and one neuron in the output layer.

A total of 240 sets of elastic modulus data containing the aggregate, asphalt binder and volumetric properties of the asphalt concrete mixes used for training and validating the neural network. The data base is randomly divided into three categories. 70% of the data is presented to the network during training, and the network is adjusted according to its error.

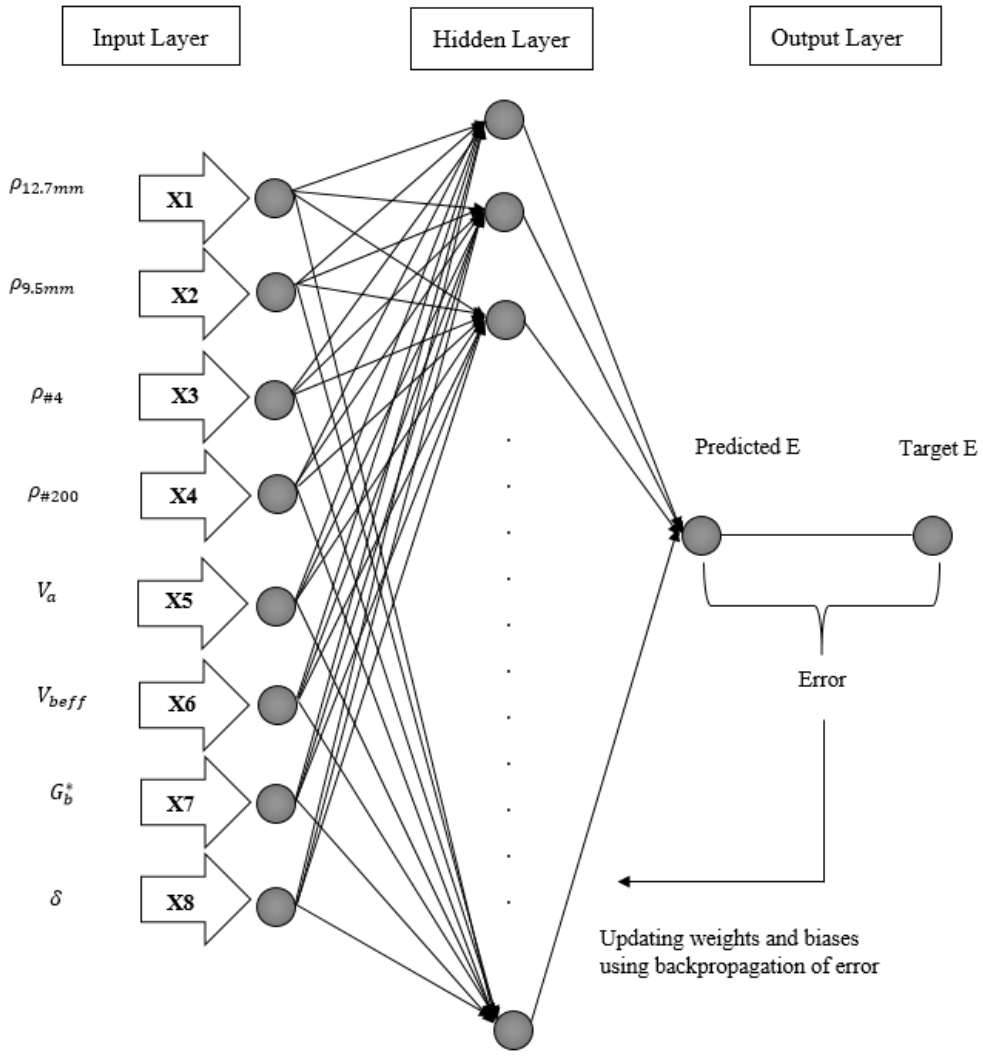

Figure 2.2 Schematic architecture of the ANN

The Levenberg-Marquardt method is chosen as the training algorithm. 15% of the data is used for the validation of fitting and to measure network generalization, and halt training when the generalization stops improving. Finally, 15% of the database is used for the testing. The testing data have no effect on the training process and provide an independent measurement of network performance. A summary of the input data with descriptive statistics obtained from the database is presented in Table 2.3.

Table 2.3 Artificial neural network input data

Variable		Values in the database			
		Maximum	Minimum	Average	Std. Dev
Asphalt Binder	Complex Modulus (Mpa)	1065.6	0	45.4	117.2
	Phase angle (degree)	79.2	28.2	52.9	11.5
Volumetric Properties	Vbeff%	5.6	4.5	5.1	0.4
	Va%	4.0	4.0	4.0	0
	% Passing 1/2"	96.4	87.2	93.9	2.6
	% Passing 3/8"	87.3	73.7	81	4.1
	% Passing #4	63.8	48.2	54.1	5.3
	% Passing #200	6.2	3.1	3.8	0.9

Accuracy of the prediction model is presented in Figure 2.3. The r-fit of 0.99 indicates that the ANN model is capable of predicting the elastic modulus value using asphalt binder, aggregate and volumetric properties. The obtained elastic modulus is being used as one of the inputs in the FE model, describing the elastic behavior of the asphalt mixture.

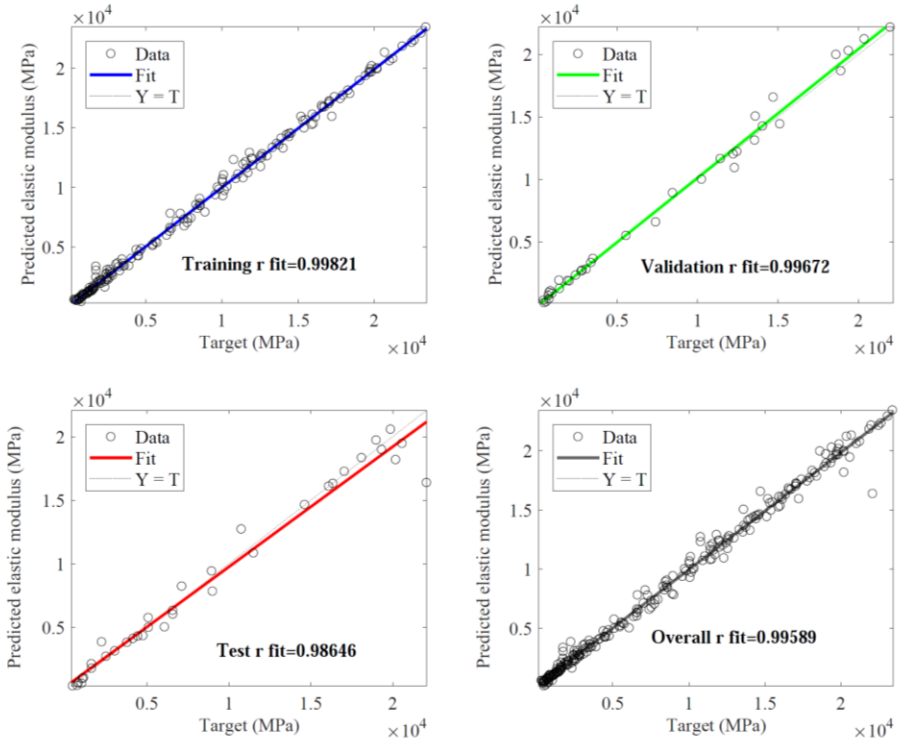

Figure 2.3 Performance of the fitting

Model geometry and meshing

The model has a cylindrical geometry having the same dimensions as the actual IDT dynamic modulus specimens. The mesh element type used for this model was from a 3D stress family, an eight-node linear brick, with reduced integration and hourglass control (C3D8R).

Loads and boundary conditions

To simulate the test, a specimen is restrained at the bottom from movement and rotation in all directions. The applied load is defined as a sinusoidal uniform pressure, applied on top of the specimen using the loading strip. Figure 2.4 illustrates the model geometry, the position of the applied load, boundary conditions and the mesh. In order to determine the load magnitude, different amounts of load amplitudes are studied and adjusted so that the observed horizontal and vertical strains in the centre area of the specimen remain between 60 and 80 and below 100 micro-strain, respectively.

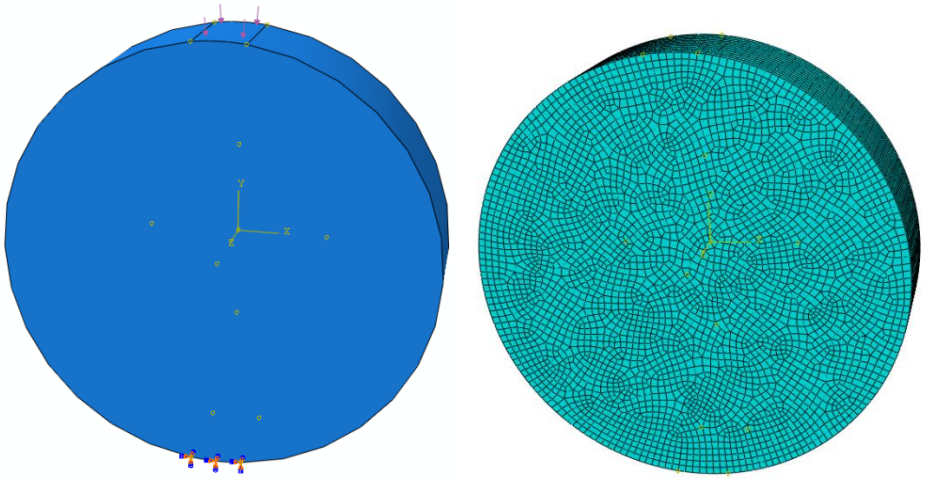

(a) *(b)*

Figure 2.4 (a) Loads and boundary condition (b) The meshed model

CHAPTER 3. RESULTS AND DISCUSSION

Results of the laboratory tests, modified Witczak model prediction and FE simulation and a comparison between them are presented in this section.

Complex shear test results

Complex shear modulus values were determined and were used to create maser curves. The master curves are presented in Figure 3.1.

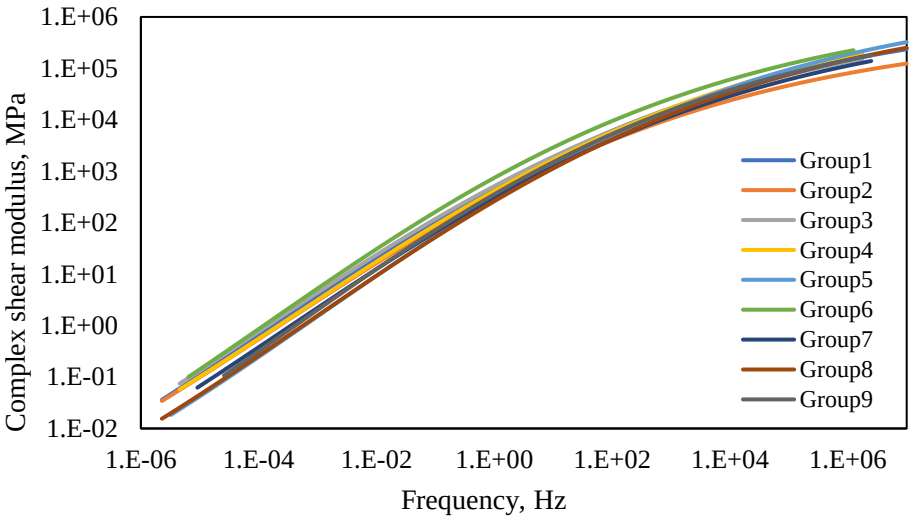

Figure 3.1 Complex shear modulus master curves

Dynamic modulus results

The average results of dynamic modulus test for three specimens per group in the IDT mode for the nine different pavement sections are presented in Table 3.1.

Table 3.1 Average dynamic modulus results for nine groups (MPa)

Group No.	Temp.	25 Hz	20 Hz	10 Hz	5 Hz	2 Hz	1 Hz	0.5 Hz	0.2 Hz	0.1 Hz
1	0.4	20425	20252	22008	18619	17501	16210	14836	13512	11995
1	17.1	12573	12510	11315	9360	7537	6399	5081	3928	3104
1	33.8	4798	4718	3462	2495	1680	1193	1000	656	502
2	0.4	14822	17293	18841	17532	15858	14445	13132	11527	10191
2	17.1	9768	9528	8905	7362	5751	4768	3934	2958	2386
2	33.8	3157	2629	2077	1691	1203	982	779	631	593
3	0.4	20128	19719	19727	18427	16927	15917	14710	13495	12285
3	17.1	15137	15679	14442	12439	10730	9330	7999	6584	5652
3	33.8	5769	5424	4419	3379	2353	1813	1394	1010	832
4	0.4	21585	20264	19523	18049	16166	14767	13283	11639	10277
4	17.1	13191	12485	11481	10044	7754	6457	5244	4008	3281
4	33.8	5083	4877	3591	2718	1897	1443	1145	820	664
5	0.4	22738	16279	16353	14882	13157	11970	10627	9074	7931
5	17.1	9634	8889	7820	6369	4802	3875	3032	2244	1638
5	33.8	3172	2882	2180	1621	1183	1005	950	750	607
6	0.4	22324	23397	21829	20659	18753	17531	16515	14680	13266
6	17.1	14264	13526	13312	11314	8720	7472	6167	4887	3921
6	33.8	5512	5241	4146	3028	1995	1520	1138	766	557
7	0.4	26413	22774	22624	21734	20130	18938	17544	15723	14373
7	17.1	13950	13122	12836	10514	8153	6782	5470	4310	3459
7	33.8	4486	4161	3377	2440	1658	1256	976	710	519
8	0.4	24299	22946	22938	21377	20027	18331	16929	15092	13813
8	17.1	12588	12151	10727	8796	7034	5822	4758	3653	2935
8	33.8	4627	4006	3347	2695	1906	4886	1320	1171	1061
9	0.4	20954	19559	20433	18470	16892	15498	14046	12499	11149
9	17.1	11719	11584	10429	8377	6339	5194	4020	2965	2147
9	33.8	4832	4195	3067	2171	1539	1198	919	614	468

Modified Witczak model

Master curves were developed for G_b* using the sigmoidal model. The model coefficients and shift factors for each group are shown in Table 3.2. These values can be used to reconstruct the curves.

Table 3.2 G* sigmoidal model coefficients and shift factors.

Group No.	δ	α	β	γ	a	b	c
1	-6.253	12.421	-0.942	0.248	0.000339	-0.113	1.825
2	-5.861	11.656	-0.949	0.257	0.000497	-0.122	1.944
3	-6.292	12.407	-0.973	0.245	0.000404	-0.118	1.906
4	-6.106	12.508	-0.836	0.241	0.000292	-0.103	1.680
5	-6.103	12.530	-0.766	0.253	0.000440	-0.115	1.840
6	-6.190	12.467	-0.979	0.254	0.000372	-0.118	1.906
7	-6.284	12.400	-0.881	0.247	0.000312	-0.105	1.710
8	-6.178	12.490	-0.792	0.250	0.000443	-0.115	1.834
9	-6.271	12.410	-0.900	0.260	0.000362	-0.111	1.800

For comparison purposes $|G_b^*|$ from lab was plotted against the predicted $|G_b^*|$ results using the sigmoidal model for each of the nine different groups as shown in Figure 3.2 (a). Figure 3.2 (b) displays an overall comparison of all the results of the groups for the lab $|G_b^*|$ versus sigmoidal predicted $|G_b^*|$. Table 3.3 shows the R^2 and correlation coefficient (R) values calculated from fitting lab $|G_b^*|$ values against $|G_b^*|$ predicted by sigmoidal model.

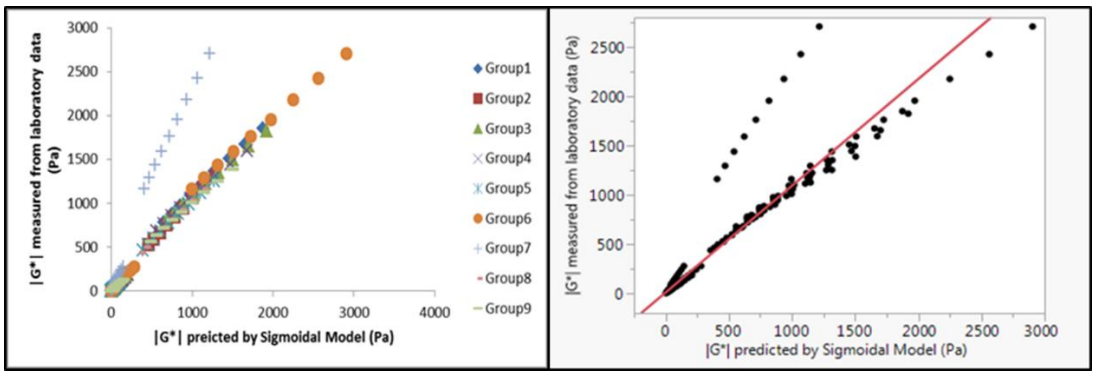

(a) (b)

Figure 3.2 Laboratory Data of |Gb*|vs. Predicted |Gb*| (a) each group, (b) all groups together.

Table 3.3 R2 and R from fitting lab |Gb*| values against sigmoidal predicted |Gb*|.

Group No.	1	2	3	4	5	6	7	8	9	All Groups
R^2	0.995	0.998	0.995	0.994	0.996	0.995	0.993	0.997	0.994	0.91
Correlation Coefficient	0.998	0.999	0.998	0.997	0.998	0.998	0.997	0.997	0.997	0.954

From the results shown, the sigmoidal model shows an extremely good fit for the experimental data of each group as well as the data from all the groups put together. This is apparent as both R and R^2 are in the range of 0.91 to 0.999. Dynamic modulus master curves were developed for E* using the sigmoidal model as well. The model coefficients and shift factors for each group's model are shown in Table 3.4.

Table 3.4 E* sigmoidal model coefficients and shift factors.

Group No.	**δ**	***α***	**β**	**γ**	***a***	***b***	***c***
1	1.617	2.778	-1.32	0.626	2.171	0.000	-1.849
2	2.363	1.938	-0.762	0.699	2.472	0.000	-2.11
3	2.073	2.288	-1.618	0.659	1.546	0.000	-2.312
4	1.957	2.465	-1.128	0.625	1.734	0.000	-1.828
5	2.51	1.855	-0.31	0.75	1.947	0.000	-1.698
6	1.145	3.301	-1.589	0.565	2.104	0.000	-1.932
7	1.274	3.217	-1.267	0.488	3.267	0.000	-2.199
8	0.79	4.046	-0.985	0.353	2.375	0.000	-1.715
9	1.345	3.041	-1.254	0.638	2.089	0.000	-1.453

To compare the sigmoidal model with the experimentally gained dynamic modulus values shifted to reduce frequencies, Figure 3.3 was created. Figure 3.3 is split into two parts (a) separated groups, and (b) all groups data pooled together. From the plots it appears that the sigmoidal model does a very good job fitting the experimental results. The R^2 and R values were determined for each group and for all data from all groups pooled together with results shown in Table 3.5.

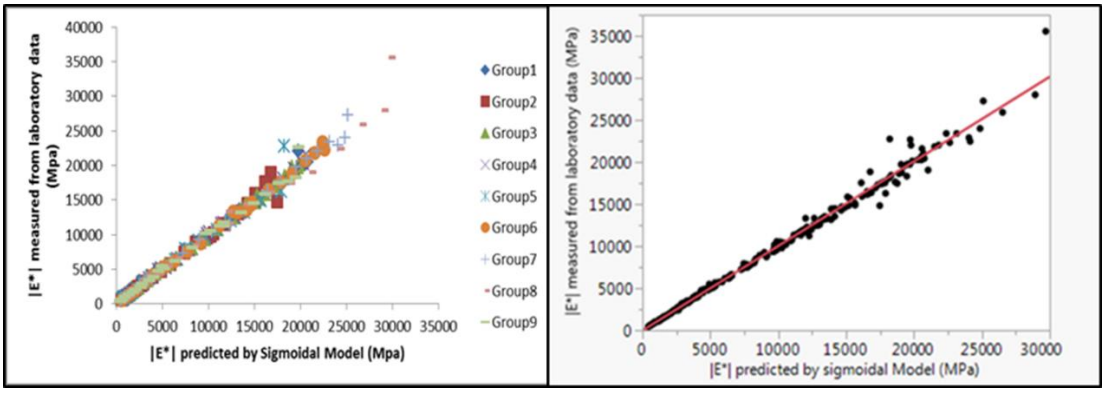

(a) (b)

Figure 3.3 Laboratory Data for |E*| vs. Predicted |E*| (a) each group, (b) all groups together.

Table 3.5 R2 and R from fitting lab |E*| values against sigmoidal predicted |E*|.

Group No.	1	2	3	4	5	6	7	8	9	All Groups
R^2	0.995	0.984	0.998	0.998	0.972	0.998	0.995	0.980	0.990	0.990
Correlation Coefficient	0.998	0.992	0.999	0.999	0.990	0.999	0.998	0.990	0.990	0.995

The sigmoidal model shows very good agreement with the experimentally shifted $|E^*|$ results from both Figure 2.3 (a) and (b) as both the R and R^2 values are in the range of 0.972 to 0.999. Using the $|G_b^*|$ master curve results in combination with volumetrics shown in Table 3.2, the dynamic modulus master curves were developed using the Modified Witczak Model. Comparison between the experimentally shifted data and Modified Witczak Model predicted data were made for each group and for all the groups pooled together. The results are presented in Figure 3.4 parts (a) and (b). From the results it is fairly clear that the Modified Witczak Model predicted results do not fit well with the experimentally shifted results for all the groups together as shown in Figure 3.4 (b). However, it is not clear from visual inspection if the Modified Witczak Model fits well or poorly with the experimentally shifted data for each individual group (Figure 3.4 (a)). To better examine the best fit models, the R and R^2 values were determined for each group and the all the groups data pooled together as shown in Table 3.6.

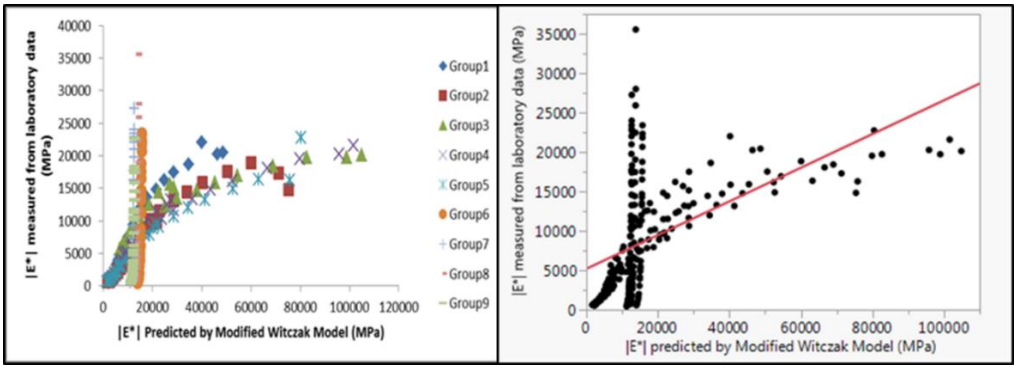

(a) (b)

Figure 3.4 Laboratory Data for |E*|vs. Predicted |E*| (a) each group, (b) all groups together.

Table 3.6 R2 and R for lab |E*| vs. |E*| predicted values by Modified Witczak model.

Group No.	1	2	3	4	5	6	7	8	9	All Groups
R^2	0.89	0.82	0.74	0.87	0.93	0.79	0.78	0.76	0.77	0.30
Correlation Coefficient	0.94	0.91	0.86	0.93	0.96	0.88	0.88	0.87	0.88	0.54

From the results shown, the Modified Witczak Model works fairly well for each group individually as the R and R^2 range from 0.74 to 0.96. However, looking at the overall fit of all the data together the R and R^2 are 0.54 and 0.30. Examining the fitted plots in Figure 3.4 does not explain what is happening, so Figure 3.5 is shown to illustrate why the R and R^2 could be low for the overall fit of all data. Figure 3.5 shows a comparison between the sigmoidal model and Modified Witczak Model against experimentally shifted data for different groups.

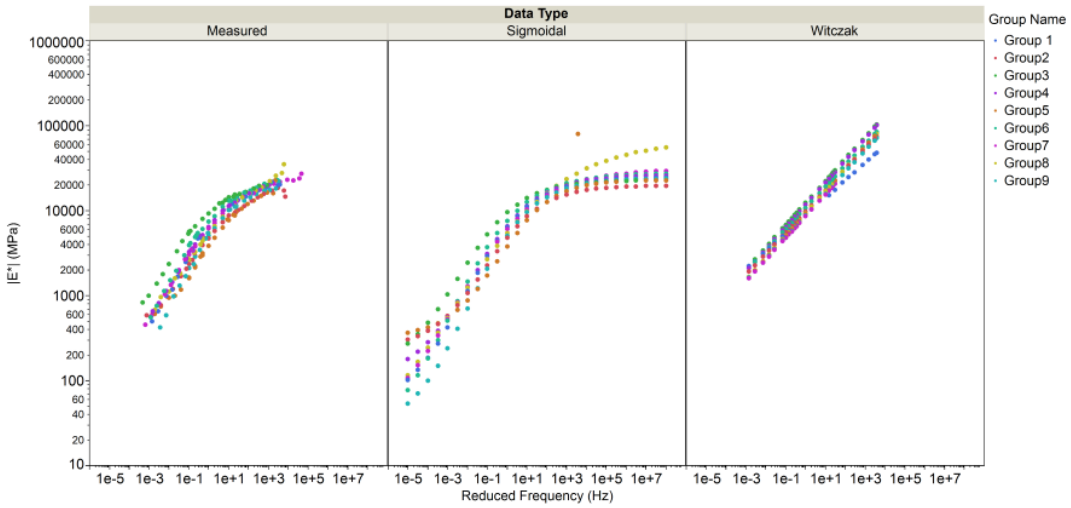

Figure 3.5 │E*│Curves for shifted Measured Data, Sigmoidal, and Modified Witczak (Witczak) fitted models.

From the resulting master curves shown in Figure 3.5 it can be seen that the Modified Witczak Model over estimates the dynamic modulus values from low to high frequencies. This is most likely due to the Modified Witczak Model creation based on historical data gained from testing 4-inch diameter by 6-inch high dynamic modulus specimens.

Finite element analysis

Figure 3.6 shows the deformed shape of asphalt concrete specimen due to sinusoidal loading with the 25 Hz frequency.

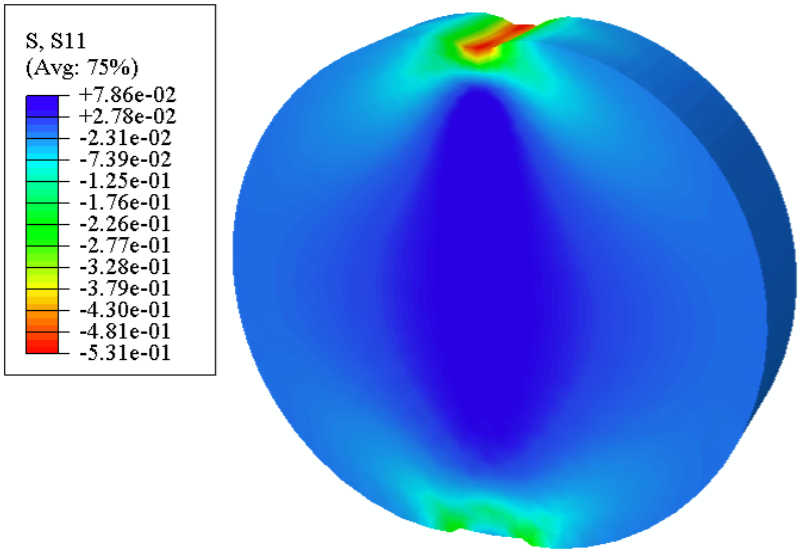

(a) Horizontal stress (σ_{xx})

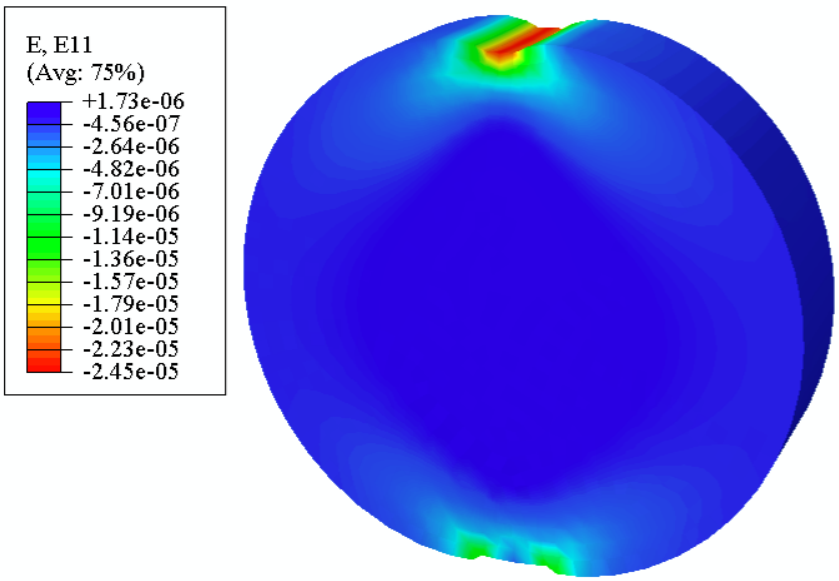

b) Horizontal strain (ϵ_{xx})

Figure 3.6 Stress, strain and deformation of deformed specimen

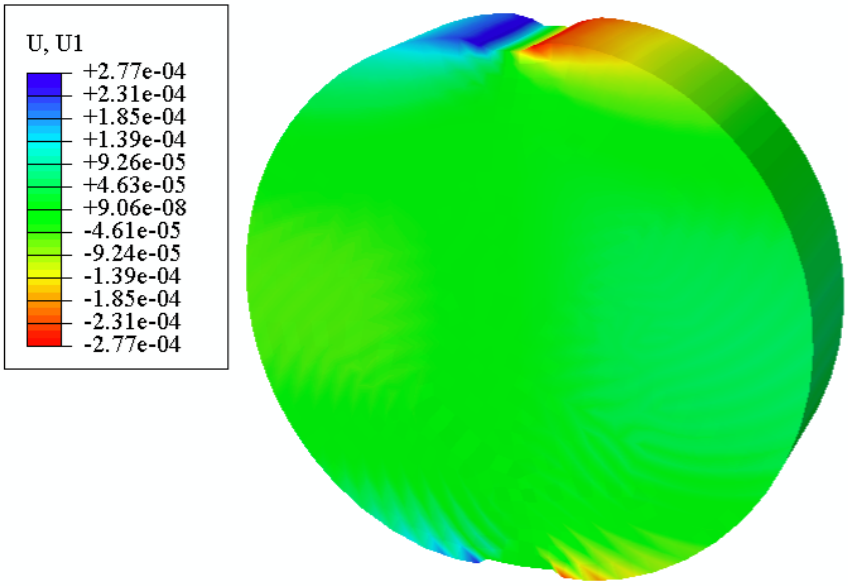

c) Horizontal deformation (U_x)

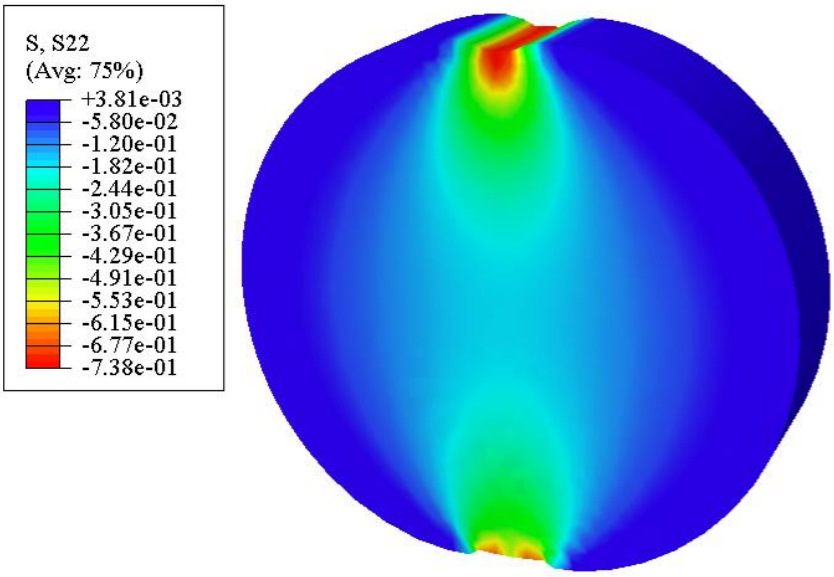

(d) Vertical stress (σ_{yy})

Figure 3.6. (Continued) Stress, strain and deformation of deformed specimen

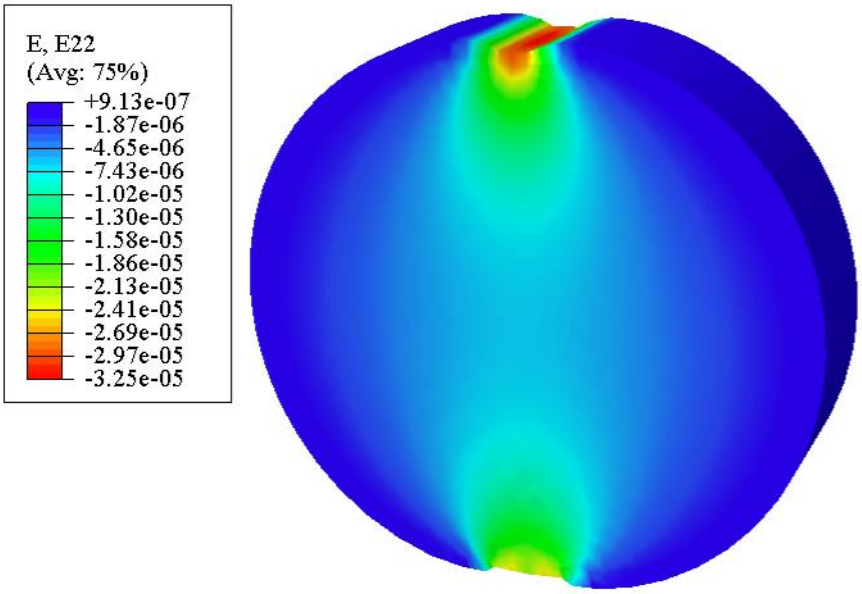

(e) Vertical strain (ϵ_{yy})

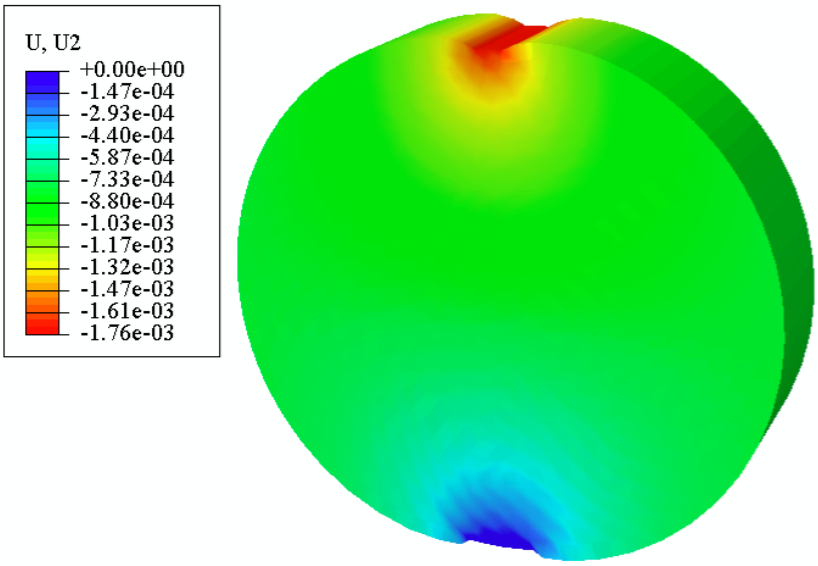

(f) Vertical deformation (U_y)

Figure3.6. (Continued) Stress, strain and deformation of deformed specimen

The calculations and data quality are based on a linear viscoelastic solution for the IDT dynamic modulus test. It should also be mentioned that all of these calculations are being done for the last 5 cycles of each frequency sweep of the laboratory test. The applied sinusoidal load in the test can be written as:

$$\boldsymbol{P = P_0(\cos \omega t + i \sin \omega t)} \tag{8}$$

where P_0 and ω = the amplitude and an the frequency of the sinusoidal load which is applied during the test. Due to the load, a test specimen will have a vertical and horizontal displacement which can be written with the following functions:

$$\boldsymbol{V(t) = V_0 \sin(\omega t - \varphi)} \tag{9}$$

$$U(t) = U_0 \sin(\omega t - \varphi) \tag{10}$$

where V_0 and U_0 are the constant amplitudes of vertical and horizontal displacement, respectively.

The dynamic modulus can be obtained from the following equation:

$$\boldsymbol{|E^*(\omega)| = \frac{2|P_0|}{\pi a d} \frac{\beta_1 \gamma_2 - \beta_2 \gamma_1}{\gamma_2 |\overline{V_0}| - \beta_2 |\overline{U_0}|}} \tag{11}$$

$\beta_1, \beta_2, \gamma_1, \gamma_2$ are geometrics coefficients. Kim calculated these coefficients for different specimen sizes and gauge lengths (Kim *et al.* 2004). After Lin (Lin *et al.* 2015), (Lin *et al.* 2016) the coefficients used in this study are calculated for a 152.4-mm specimen diameter and a 65-mm gauge length using equations 9 to 16 (Hondros 1959) and presented in Table 3.7.

$$\boldsymbol{\beta_1 = -\int_{-l}^{l} n(y) dy - \int_{-l}^{l} m(y) dy} \tag{12}$$

$$\beta_2 = \int_{-l}^{l} n(y)dy - \int_{-l}^{l} m(y)dy \tag{13}$$

$$\boldsymbol{\gamma_1 = \int_{-l}^{l} f(x)dx - \int_{-l}^{l} g(x)dx} \tag{14}$$

$$\boldsymbol{\gamma_2 = \int_{-l}^{l} f(x)dx + \int_{-l}^{l} g(x)dx} \tag{15}$$

where,

$$\boldsymbol{n(y) = \tan^{-1}\left(\frac{1+\frac{y^2}{R^2}}{1-\frac{y^2}{R^2}}\tan\alpha\right)} \tag{16}$$

$$\boldsymbol{m(y) = \frac{\left(1-\frac{y^2}{R^2}\right)\sin 2\alpha}{1-2\left(\frac{y^2}{R^2}\right)\cos 2\alpha + \frac{y^4}{R^4}}} \tag{17}$$

$$f(x) = \frac{\left(1 - \frac{x^2}{R^2}\right)\sin 2\alpha}{1 - 2\left(\frac{x^2}{R^2}\right)\cos 2\alpha + \frac{x^4}{R^4}} \quad (18)$$

$$\boldsymbol{g(x) = \tan^{-1}\left(\frac{1 - \frac{x^2}{R^2}}{1 + \frac{x^2}{R^2}}\tan\alpha\right)} \quad (19)$$

where, x = the horizontal distance from the specimen centre; y = the vertical distance from the centre of specimen; R = the specimen radius ; α = the radial angle, and *l* = the half of the gauge length.

Table 3.7 Geometrics coefficients

Specimen Diameter (mm)	**Gauge Length (mm)**	**β_1**	**β_2**	**γ_1**	**γ_2**
152.4	65	0.0262	-0.0078	0.0063	0.0206

Vertical and horizontal stresses (S_{22}, S_{11}) and deformations (U2, U1) of the sample under the applied load were obtained for different loading frequencies. Complex modulus values of nine different pavement sections are then calculated for each loading frequency using equation 20.

$$\boldsymbol{E^* = \frac{S_{11} - \nu S_{22}}{E_{11}}} \quad (20)$$

where, S_{11}= the horizontal stress along the x-axis; S_{22} = the vertical stress along the x-axis, and E_{11} = the horizontal strain along the x-axis. The obtained modulus from equation 20 is the complex modulus of the material along the x-axis which is assumed to be the same as the complex modulus along the y-axis.

According to equation 2, the dynamic modulus value will be the amplitude of the complex modulus wave.

$$\boldsymbol{E^*} = |\boldsymbol{E^*}|.\boldsymbol{e^{i\phi}} \tag{21}$$

where, E^* = the complex modulus; $|E^*|$ = the dynamic modulus; e = the exponential function; i = the imaginary component of the complex modulus, and ϕ = the phase angle.

A comprehensive comparison is done between the simulation results and the laboratory data. Figure 3.7 shows a comparison of master curves created using experimental results versus simulation results. For all nine groups of specimens, the FE model was able to predict the value of dynamic modulus.

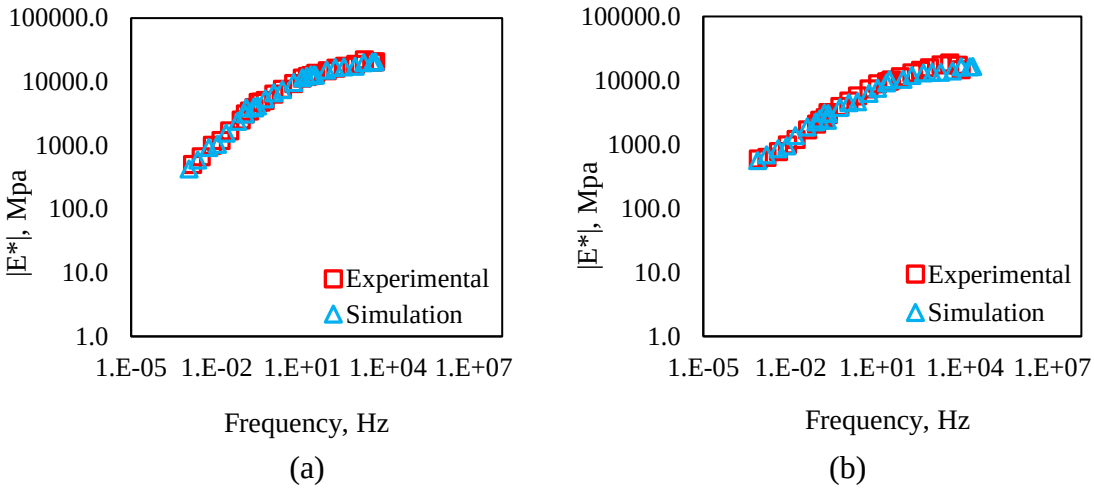

Figure 3.7 Comparison of master curves created using experimental results and simulation results for 9 different pavement sections

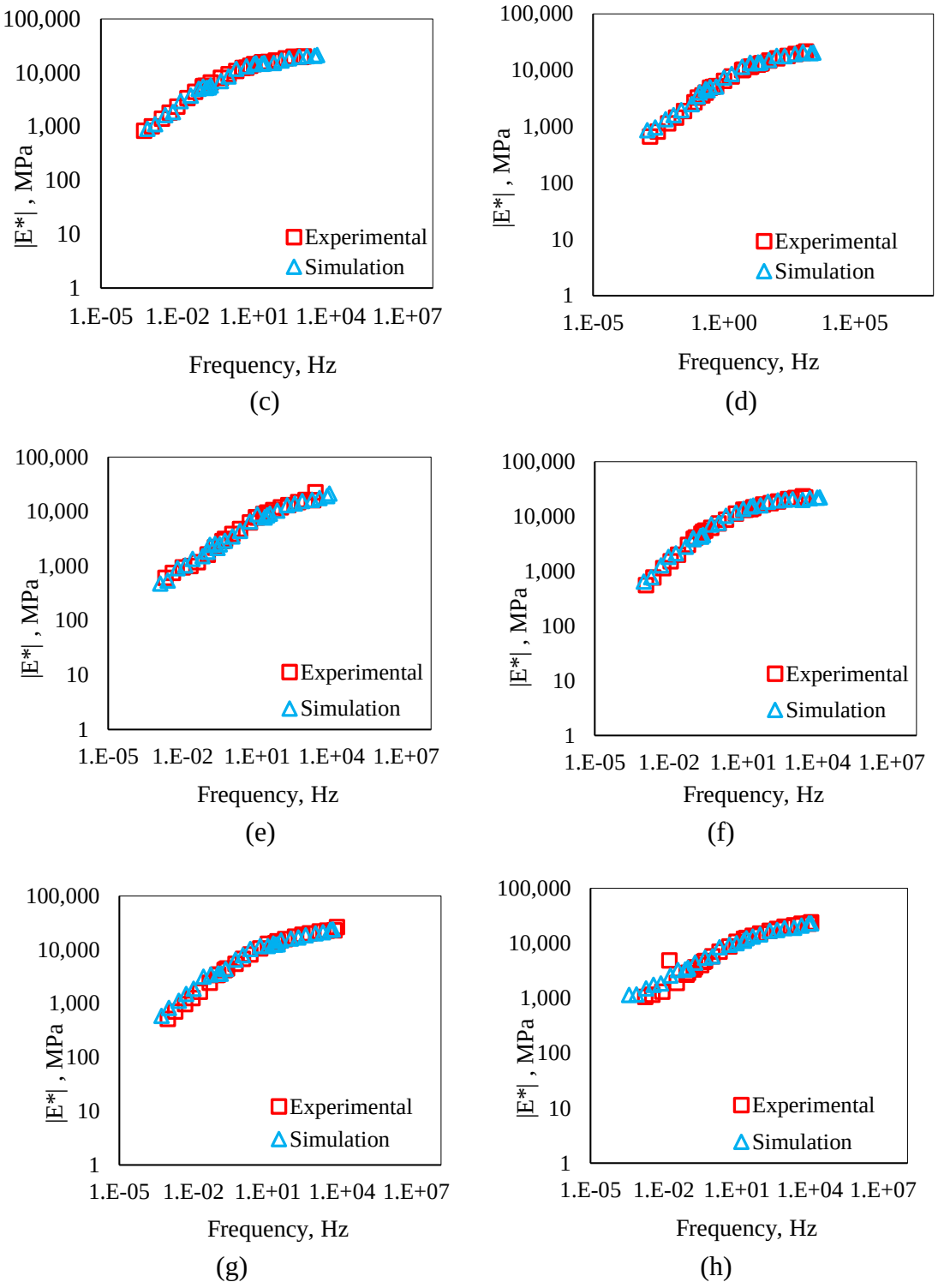

Figure 3.7 (Continued) Comparison of master curves created using experimental results and simulation results for 9 different pavement sections

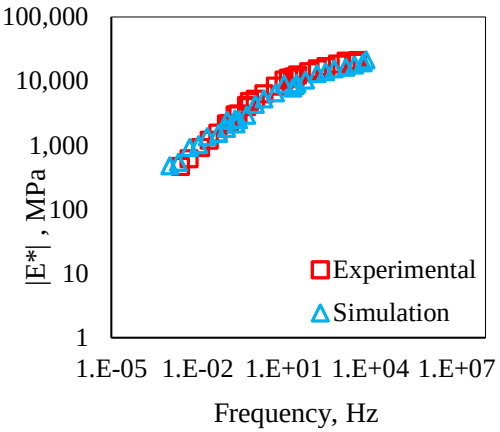

(i)

Figure 3.7 (Continued) Comparison of master curves created using experimental results and simulation results for 9 different pavement sections

Element size is an important factor in determining the accuracy of solution in FE method. To converge the solution to the correct value, the mesh should be properly discretized or a proper order element should be selected. In order to examine the ability of selecting a proper mesh by balancing accuracy of the solution as well as computational efficiency, a mesh convergence study is performed using five different mesh sizes including 10, 7.5, 5, 2.5 and 2 mm. The result of the convergence study for the first group of asphalt mixtures is presented in this section. Figure 3.8 represents a log-log scale of the relative error (%) versus the number of elements for different loading frequencies. Based on the convergence study results, the relative error will converge to a specific value by increasing the number of elements or decreasing the mesh size.

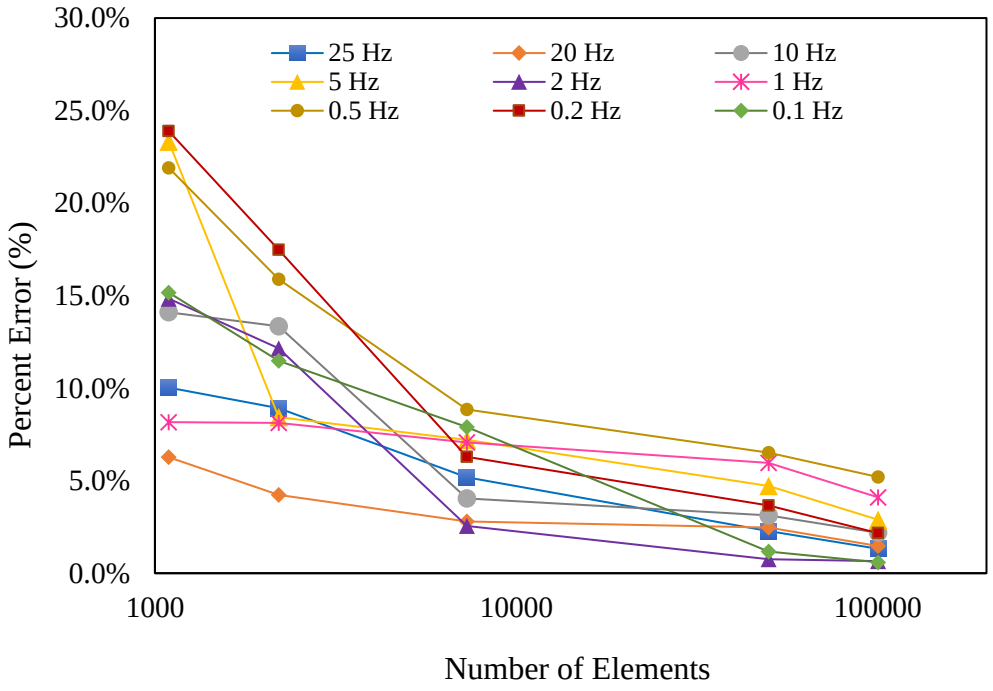

Figure 3.8 Convergence study results

The relative errors between simulation results and laboratory data for different loading frequencies and for different pavement sections were less than 20%, which indicates that FE modelling is a capable tool to estimate dynamic modulus and performance evaluation of asphalt concrete. Larger amount of error was observed for groups 7, 8 and 9 which means that the assumption of homogeneity for asphalt mixture is not accurate although it will give a rough estimation of dynamic modulus values.

Model validation

The decomposition of the variability in the observations through an analysis of variance identity is a purely algebraic relationship. However, the use of the partitioning to formally test for no differences in treatment means requires that certain assumptions be

satisfied. According to these assumptions, the observations are adequately described by the model presented by equation 22.

$$\boldsymbol{y_{ij} = \mu + \tau_i + \epsilon_{ij}} \tag{22}$$

where, y_{ij} = the observation j from treatment i; μ = the overall mean; τ_i = the ith treatment effect, and ϵ_{ij} = the random error. It is assumed that the error is normally and independently distributed with mean zero and constant but unknown variance σ^2.

Violation of the basic assumptions and model adequacy can be easily investigated by the examination of residuals. The residual for observation j in treatment i is defined by equation 23.

$$\boldsymbol{e_{ij} = y_{ij} - \widehat{y_{ij}}} \tag{23}$$

where, $\widehat{y_{ij}}$ = the predicted value of the corresponding observation y_{ij}.

Through analysis of the residuals, many types of model inadequacies and violations of the underlying assumptions can be discovered. If the model is adequate, the residuals should contain no obvious patterns (Montgomery 2012). The residual plot presented in the Figure 3.9 Containing no obvious pattern by the residual plot is supporting the assumption of equal variances.

Checking the normality assumption of the errors can be made by constructing a normal probability plot of the residuals. If the underlying error distribution is normal, this plot will resemble a straight line (Montgomery 2012). The normal probability plot of the residuals is presented in Figure 3.10. The data points are not too far away from a straight line.

So, the normality assumption is satisfied. Figure 3.11 represents the linear relationship between laboratory data and simulation results which has a R^2 value of 0.98.

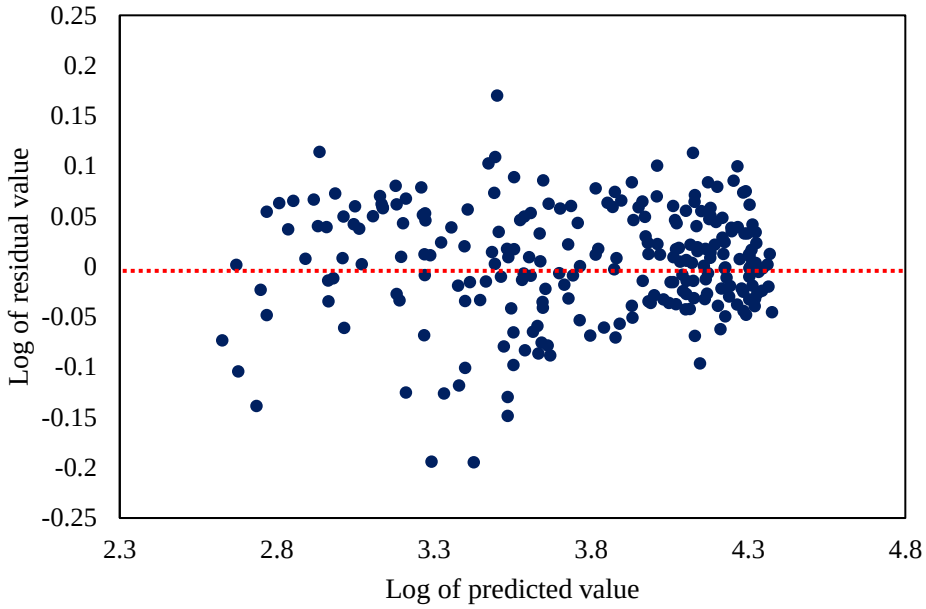

Figure 3.9 Log of residual versus log of predicted values of dynamic modulus

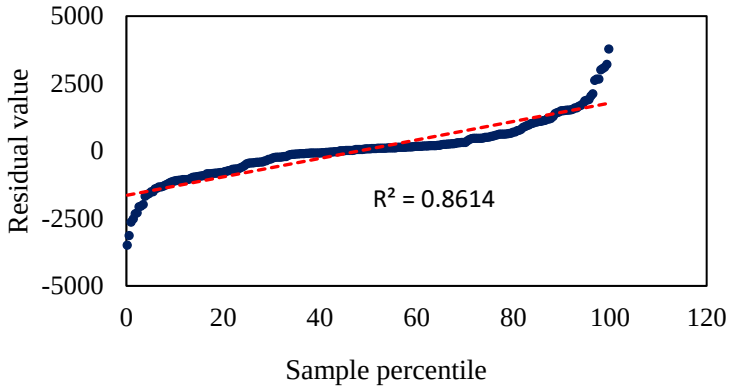

Figure 3.10 Normal probability plot of residuals

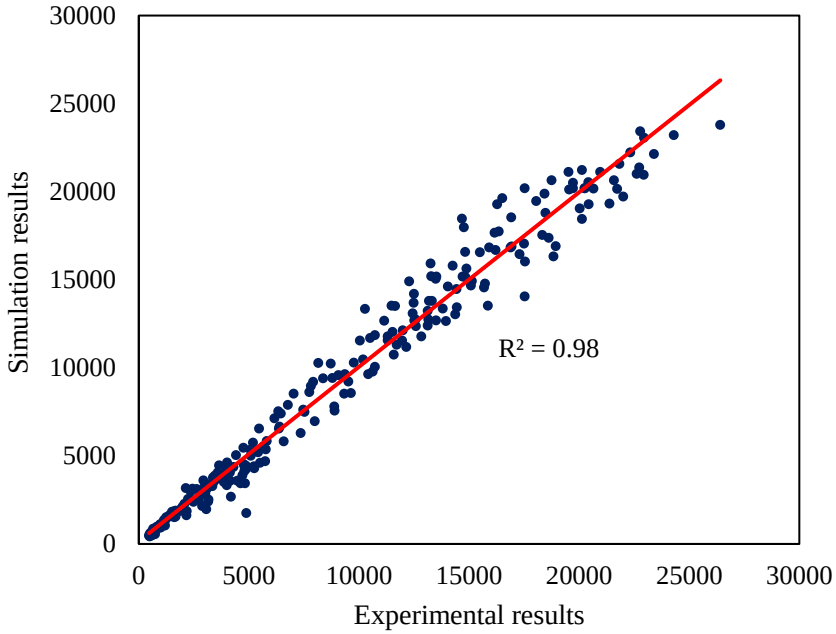

Figure 3.11 Experimental results versus simulation results

CHAPTER 4. CONCLUSIONS AND RECOMMENDATIONS

The IDT dynamic modulus test results showed that all nine mix groups have very high stiffness values. The R^2 and R values gained from fitting experimental results against predicted data using the sigmoidal model were close to 1, and thus means the sigmoidal model can be developed and used to predict both $|E^*|$ and $|G_b^*|$ values very well. For the IDT mode of testing, although the Modified Wiczak model can predict $|E^*|$ values using $|G_b^*|$ and other inputs for the more commonly used uniaxial test configuration for determining dynamic modulus values, it is not as accurate in predicting IDT $|E^*|$ values as the sigmoidal model. Due to the ability of IDT dynamic modulus test to more accurately measure the dynamic modulus in asphalt concrete layers collected from field cores, the Modified Witczak Model should be modified for IDT mode in future studies.

The present study used the experimental data of complex shear modulus, aggregate gradation, and volumetric properties of asphalt mixture to estimate the dynamic modulus value by means of finite element method (FEM). In order to define the elastic behaviour of asphalt mixture, back-calculation of elastic modulus was done using ANN. The assumption of dynamic modulus test in indirect tension mode is based on linear viscoelastic solution which means the material is assumed to remain in the linear viscoelastic range of behavior. Although the simulation would be limited to predict the material performance in the linear viscoelastic range, this is not a limitation of the model. In order to evaluate the performance of asphalt concrete using dynamic modulus test results, creating a smooth and complete master curve is desired which can be obtained by using FE modeling. More testing of different mixtures and model improvement is needed in order to further reduce the relative error. All of the specimens used in the finite element modeling were from the State of

Minnesota. More variety in asphalt concrete specimens could be helpful in model modification.

Limitations of the study

Although doing FE modeling could save time and money, a lot of computational time is needed to do the simulation. The assumption of homogeneity for asphalt mixtures undoubtedly will lead to some error, in order to overcome this weakness, the model should be modified using different elastic modulus values in the x and y directions (tension and compression, respectively).

REFERENCES

AASHTO T 342-11, 2012. *AASHTO T 342-11 Determining Dynamic Modulus of Hot Mix Asphalt (HMA)*. American Association of State Highway and Transportation Officials.

AASHTO TP 79-13, 2013. AASHTO TP 79-13 Determining the Dynamic Modulus and Flow Number for Asphalt Mixtures Using the Aphalt Mixtures Performance Tester. *American Association of State Highway and Transportation Officials*, 1–19.

Akbulut, H. and Aslantas, K., 2005. Finite element analysis of stress distribution on bituminous pavement and failure mechanism. *Materials & Design*, 26 (4), 383–387.

Aslani, M. and Asla, R., 2010. A Novel Hybrid Simplex-Genetic Algorithm For The Optimum Design Of Truss Structures. *Lecture Notes in Computer Science*, II.

ASTM D2172, 2011. Standard Test Methods for Quantitative Extraction of Bitumen From Bituminous Paving Mixtures. *American Society for Testing and Materials*, i, 1–13.

ASTM D7906-14, 2014. *ASTM D7906-14 Standard Practice for Recovery of Asphalt from Solution Using the Toluene and the Rotary Evaporator*. American Society for Testing and Materials.

ASTM D 3497-79, 1995. *Standard Test Method for Dynamic Modulus of Asphalt Mixtures*. American Society for Testing and Materials.

Breakah, T. and Williams, R.C., 2013. Stochastic Finite Element Analysis of Moisture Damage in Hot Mix Asphalt. *Materials and Structures*, 48, 93–106.

Breakah, T., Williams, R.C., Schaefer, V.R., and Wang, K., 2009. Stochastic Finite element Analysis of Moisture Damage in Hot Mix Asphalt.

Brinson, H.F. and Brinson, L.C., 2015. *Polymer engineering science and viscoelasticity: An introduction, Second edition*. Polymer Engineering Science and Viscoelasticity: An Introduction.

Collop, A.C., Scarpas, A.T., Kasbergen, C., and Bondt, A. De, 2003. Development and Finite Element Implementation of Stress-Dependent Elastoviscoplastic Constitutive Model with ... OF A STRESS DEPENDENT ELASTO-VISCO-PLASTIC. *Transportation Research Record*, (January).

Documentation, Abaqus. 'Version 6.14-2.', 2014. *Dassault Systémes Simulia Corp., Providence, RI.*

Dougan, C.E., Stephens, J.E., Mahoney, J., and Hansen, G., 2003. Dynamic Modulus Test Protocol - Problems and Solutions. *FHWA Report*.

Duncan and M.C, 1968. Finite Element Analysis of Pavements. *Transportation Research Record*, 228, 18–33.

Elseifi, M. a., Al-Qadi, I.L., and Yoo, P.J., 2006. Viscoelastic Modeling and Field Validation of Flexible Pavements. *Journal of Engineering Mechanics*, 132 (2), 172–178.

Ghasemi, P., Aslani, M., Rollins, D.K., Christopher Williams, R., and Schaefer, V.R., 2018. Modeling Rutting Susceptibility Of Asphalt Pavement Using Principal Component Pseudo Inputs In Regression And Neural Networks. *International Journal of Pavement Research and Technology*.

Ghasemi, P., Podolsky, J., Christopher Williams, R., and Dave, E., 2016. Performance Evaluation of Coarse-Graded Field Mixtures Using Dynamic Modulus Results Gained from Testing in the Indirect Tension Mode. *In*: *International Conference on Transportation and Development 2016: Projects and Practices for Prosperity - Proceedings of the 2016 International Conference on Transportation and Development*.

Herzog, M., Gilg, A., Paffrath, M., Rentrop, P., and Wever, U., 2008. Intrusive versus Non-Intrusive Methods for Stochastic Finite Element. *From Nano to Space*, 161–174.

Hondros, G., 1959. The Evaluation of Poisson's Ratio and the Modulus of Materials of Low Tensile Resistance by the Brazilian (Indirect Tensile) Test with Particular Reference to Concrete. *Australian Journal of Applied Science*, 10, 243–268.

Kartam, Nabil. Flood, I., 1994. Neural Netwroks in Civil Engineering: Principal and Understanding. *Journal of Computing in Civil Engineering*, 8 (2), 131–148.

Kartam, N., 1994. Neural Netwroks in Civil Engineering: Systems and Application. *Journal of Computing in Civil Engineering*, 8 (2), 149–162.

Kim, Y., Seo, Y., King, M., and Momen, M., 2004. Dynamic Modulus Testing of Asphalt Concrete in Indirect Tension Mode. *Transportation Research Record*, 1891 (1), 163–173.

Kim, Y.R. and Wen, H., 2002. Fracture energy from indirect tension testing. *Asphalt Paving Technology 2002, March 18, 2002 - March 20, 2002*, 71 (August), 779–793.

Li, X. and Williams, R.C., 2015. A Practical Dynamic Modulus Testing Protocol. *Journal of Testing and Evaluation*, 40 (1), 1–7.

Lin, S., Ashlock, J.C., and Williams, R.C., 2016. Nondestructive quality assessment of asphalt pavements based on dynamic modulus. *Construction and Building Materials*, 112, 836–847.

Lin, S., Ashlock, J.C., Williams, R.C., Lee, H.D., Kim, H., and Nash, J., 2015. *Assessment of Nondestructive Testing Technologies for Quality Control/Quality Assurance of Asphalt Mixtures*. Ames, IA.

Lytton, R.L., Uzan, J., Fernando, E.G., Roque, R., Hiltunen, D., and Stoffels, S.M., 1993. Development and validation of performance prediction models and specifications for asphalt binders and paving mixes. SHRP-A-357, 552.

MATLAB, 2012. Matheworks, T., 2012. Matlab 2012b. ,.

Mitchell, M.R., Link, R.E., Levenberg, E., and Shah, A., 2008. Interpretation of Complex Modulus Test Results for Asphalt-Aggregate Mixes. *Journal of Testing and Evaluation*, 36 (4), 101577.

Montgomery, D.C., 2012. *Design and Analysis of Experiments*. 8th ed. Design. Tempe, Arizona.

Raad, L. and Figueroa, J.L., 1980. Load Response of Transportation Support systems. *Transportation Engineering Journal of ASCE*, 106, 111–128.

Rahami, H., Kaveh, A., Aslani, M., and Asl, R.N., 2011. A hybrid modified genetic-nelder mead simplex algorithm for large-scale truss optimization. *International Journal of Optimization in Civil Engineering*, 1 (January), 29–46.

Saltan, M. and Sezgin, H., 2007. Hybrid neural network and finite element modeling of sub-base layer material properties in flexible pavements. *Materials and Design*, 28 (5), 1725–1730.

Saltan, M., Tigdemir, M., and Karasahin, M., 2002. Artificial Neural Network Application for Flexible Pavement Thickness Modeling. *Turkish Journal of Engineering, Environment and Science*, 26, 243–248.

Schapery, R. a. and Park, S.W., 1999. Methods of interconversion between linear viscoelastic material functions. Part II—an approximate analytical method. *International Journal of Solids and Structures*, 36 (11), 1677–1699.

Schwartz, C.W., 2005. Evaluation of the Witczak Dynamic Modulus Prediction Model.

Standard Test Method for Determining the Complex Shear Modulus (G *) Of Bituminous Mixtures Using Dynamic Shear Rheometer, 2016. *American Society for Testing and Materials*, (Reapproved 2014), 1–11.

Williams, M.L., Landel, R.F., and Ferry, J.D., 1955. The Temperature Dependence of Relaxation Mechanisms in Amorphous Polymers and Other Glass-forming Liquids. *Journal of American chemical society*, 77 (12), 3701–3707.

Williams, R.C., Schaefer, V.R., and Wang, K., 2009. Stochastic finite element analysis of moisture damage in hot mix asphalt by Tamer M . Breakah A dissertation submitted to the graduate faculty in partial fulfillment of the requirements for the degree of DOCTOR OF PHILOSOPHY Major : Civil Engineering (Ci.

Witczak, M.W. and El-Basyouny, M.M., 2004. *NCHRP Report 1-37A- Guide for*

Mechanistic-Empirical Design of New and Rehabilitated Pavement Structures. Appendix A: Calibration of Permamnent Deformation Models For Flexible Pavements. Transportation Research Board, Washington, DC.

Witczak, M.W., Kaloush, K., Pellinen, T., El-Basyouny, M., and Quintus, H. Von, 2002. *Simple Performance Test for Superpave Mix Design*. Design. Transportation Research Board, Washington, D.C.